Activity and selectivity of a nanostructured CuO/ZrO_2 catalyst in the steam reforming of methanol

H. Purnama[a], F. Girgsdies[a], T. Ressler[a,*], J.H. Schattka[b], R.A. Caruso[b], R. Schomäcker[c], and R. Schlögl[a]

[a]*Fritz-Haber-Institut der MPG, Abteilung Anorganische Chemie, Faradayweg 4-6, 14195 Berlin, Germany*
[b]*Max-Planck-Institut für Kolloid- und Grenzflächenforschung, Abteilung Kolloidchemie, MPI-KG 14424 Potsdam, Germany*
[c]*Institut für Chemie, TU Berlin, Sekr. TC-8, Straße des 17. Juni 124, 10623 Berlin, Germany*

Received 30 September 2003; accepted 28 January 2004

Steam reforming of methanol for production of hydrogen can be carried out over copper based catalyst. In the work presented here, the catalytic properties of a CuO/ZrO_2 catalyst (8.5 wt%) synthesised by a templating technique were investigated with respect to activity, long term stability, CO formation, and response to oxygen addition to the feed. The results were obtained using a fixed bed reactor and compared to a commercial methanol synthesis catalyst $CuO/ZnO/Al_2O_3$. It is shown that, depending on the time on stream, the temporary addition of oxygen to the feed has a beneficial effect on the activity of the CuO/ZrO_2 catalyst. After activation, the CuO/ZrO_2 catalyst is found to be more active (per copper mass) than the $CuO/ZnO/Al_2O_3$ system, more stable during time on stream (measured up to 250 h), and to produce less CO. Structural characterisation by means of X-ray powder diffraction (XRD) and X-ray absorption spectroscopy (XAS) reveals that the catalyst (as prepared) consists of crystalline, tetragonal zirconia with small domain sizes (about 60 Å) and small/disordered crystallites of CuO.

KEY WORDS: methanol steam reforming; template technique; Cu/ZrO_2; O_2 pulse; CO formation.

1. Introduction

Using methanol as a hydrogen source for fuel-cell applications is a favourable solutions to supply hydrogen on board in comparison to other hydrocarbon fuels, because of the following reasons: low temperature (250 °C) in steam reforming of methanol (SRM), high hydrogen to carbon ratio, low CO formation, and zero emission of NO_x, SO_x. A comparative study of different fuels for on-board hydrogen production for fuel-cell-powered automobiles has been carried out by Brown [1]. Possible processes for hydrogen production from methanol are decomposition, steam reforming, partial oxidation, and combined reforming (also called oxidative steam reforming) of methanol [2–5]. A higher hydrogen yield is obtained in steam reforming compared to partial oxidation and oxidative steam reforming. The production of CO in SRM using a commercial $CuO/ZnO/Al_2O_3$ catalyst is significantly lower compared to the CO production during decomposition of methanol [6], but somewhat higher than in oxidative steam reforming [2,4]. Commercial copper based catalysts with the composition $CuO/ZnO/Al_2O_3$ are used for methanol synthesis. Thus, several studies on the use of this type of industrial catalyst for SRM have been published recently [2,4,6,7]. Two main problems using this catalyst system are the poor long term stability and the formation of CO as a byproduct. CO poisons the Pt electrode of a fuel cell, even at a very low concentration [8,9]. A number of copper based catalysts promoted with different metal oxides Cu/Zn [4,10–14], Cu/Cr [4,10,13,15], Cu/Mn [10,16], Cu/Zr [4,13,15,17] have been investigated recently. Here, we present a study on the catalytic properties of a novel CuO/ZrO_2 catalyst. In order to improve the activity, long term stability, and reduced CO formation, a catalyst consisting of copper supported on ZrO_2 was synthesised using a polymer templating technique. The morphology and porosity of zirconia can be readily controlled by the templating procedure, resulting in a nanostructured material with high surface area. The small copper particles formed during reduction of the catalyst stay well separated by the ZrO_2 support, preventing sintering and loss of copper surface area with time on stream. The catalytic activity was determined in a fixed bed reactor using gas chromatography to measure the concentration of gases and liquids in the product stream. A commercial $CuO/ZnO/Al_2O_3$ catalyst (about 50 wt% Cu) was employed for comparison.

* To whom correspondence should be addressed.
E-mail: ressler@fhi-berlin.mpg.de

2. Experiment

2.1. Catalyst preparation

For the preparation of the catalyst a templating procedure was applied. At first, a porous polymer gel was formed by radical polymerisation of organic monomers in a highly concentrated surfactant solution [18–21]. Subsequently, the gel was used as the template in a sol–gel nanocoating process [22,23].

1011-372X/04/0400–0061/0 © 2004 Plenum Publishing Corporation

2.1.1. Materials

The surfactant Tween 60 ® (T60, polyoxyethylene(20) sorbitan monostearate), the organic monomers acrylamide (AA), glycidylmethacrylate (GMA) and ethylene glycol dimethacrylate (EGDMA) as well as the radical initiator potassium persulfate (KPS) were purchased from Aldrich. Zirconium(IV) propoxide (ZrP, 70% in 1-propanol) and copper(II) acetylacetonate ($CuAcac_2$) were also obtained from Aldrich. All chemicals were used as received. The water employed during the preparation was prepared in a three-stage Millipore purification system (Milli-Q Plus 185) resulting in a resistivity higher than 18 MΩ cm.

2.1.2. Polymer gel preparation

For the preparation of the polymer gel 25 g of the structure directing surfactant, T60, were dissolved in 50.00 mL of water. The monomers (6.25 g AA and 6.25 g GMA) were added to this homogeneous solution. Upon addition of 2.51 g of EGDMA as a crosslinker, the solution became turbid. The initiator (0.63 g KPS) was dissolved in the prepared mixture, which was then poured into test tubes. Polymerisation was carried out at 60 °C. After 16 h the resulting gel was taken out of the test tubes and cut into disks. The surfactant was removed by soxhlet extraction (ethanol, 2 days) and subsequent washing with water. Finally, the gel was transferred into 2-propanol.

2.1.3. Sol-gel nanocoating

20.0 g ZrP and 2.0 g $CuAcac_2$ were stirred over night. The resulting dark blue solution was nearly saturated with the copper salt. The polymer gels were initially soaked in this solution over night and then in a hydrolysis solution for 24 h. The hydrolysis solution was prepared from equal volumes of water and 2-propanol and saturated with $CuAcac_2$ by stirring it with an excess of the salt for several hours; the undissolved salt was removed by decanting the supersaturated solution. After drying, the polymer gel was removed from the metal oxide by heating the hybrid material over 2 h up to 500 °C under a nitrogen atmosphere; then the gas was switched to oxygen and the temperature was maintained for 10 h.

2.2. Structural characterisation

The X-ray diffraction (XRD) measurements were performed on a STOE STADI P diffractometer ($CuK\alpha_1$ radiation, curved Ge monochromator) in transmission geometry with a curved position sensitive detector. X-ray absorption spectroscopy (XAS) data were collected at beamline X1 at the Hamburg Synchrotron Radiation Laboratory HASYLAB. The spectra were taken at the CuK edge in transmission mode using a Si(111) double crystal monochromator. 10 mg of sample were mixed with 30 mg of hexagonal boron nitride (BN) and pressed with a force of one ton into a 5 mm in diameter self-supporting pellet. X-ray absorption fine structure (XAFS) analysis was performed using the software package WinXAS v2.3 [24]. Background subtraction and normalisation were carried out by fitting linear polynomials to the pre-edge and the post-edge region of an absorption spectrum, respectively. The extended X-ray absorption fine structure (EXAFS) $\chi(k)$ was extracted by using cubic splines to obtain a smooth atomic background, m0(k). The radial distribution function FT($\chi(k)$) was calculated by Fourier transforming the k^3-weighted experimental $\chi(k)$ function, multiplied by a Bessel window, into the R space. EXAFS data analysis was performed using theoretical backscattering phases and amplitudes calculated with the ab-initio multiple-scattering code FEFF7. [25] EXAFS refinements were performed in R space to magnitude and imaginary part of a Fourier transformed k^3-weighted experimental $\chi(k)$. Structural parameters determined by a least-squares EXAFS refinement of a Keggin model structure to the experimental spectra are (i) one E0 shift for oxygen and copper backscatterer, (ii) Debye–Waller factors for single-scattering paths, (iii) distances of single-scattering paths. Coordination numbers (CN) and S_0^2 were kept invariant in the refinement.

2.3. Kinetic studies

2.3.1. Reactor setup

SRM was performed at atmospheric pressure in a tubular stainless steel reactor (10 mm i.d.). The reactor was placed in an aluminium heating block equipped with six cartridge heaters with 125 watt each. The temperature of the reactor was regulated by PID controler of the cartridge heaters. Two thermocouples of type J (Fe versus. (Cu + 43%Ni)), one in the aluminium block, the other one in the catalyst bed, were used.

2.3.2. Catalytic measurements

For SRM the catalyst powder was first diluted with five times its weight of hexagonal BN and then the mixture was pressed using a cylinder stamp with a diameter of 29 mm. One gram of the mixture was put into the cylinder stamp and was pressed at 200 bar for 4 min, the pressing was repeated three times for each pellet. The pellet was then crushed into smaller particles that were sieved to obtain a fraction with defined particle size. The catalyst was supported by a stainless steel fixed fine mesh grid. For flow conditioning, inert Pyrex beads of the catalyst's size (0.85–1.0 mm) were placed on top and below the catalyst bed. A commercial $CuO/ZnO/Al_2O_3$ catalyst from Süd-Chemie (approximately 50 wt% Cu) [16] was used as a reference catalyst. The reactants, water and methanol, were introduced into the reactor in a molar ratio of 1 and at a liquid flow rate of 0.07 mL/min by means of an HPLC pump. Prior

to the activity measurements, the catalyst was activated at 250 °C in the reaction mixture. Non-condensable product gases were separated from unreacted water and methanol by passing the exhaust gases through a series of cold traps. The dry effluent gases which contain hydrogen, carbon dioxide and carbon monoxide were analysed using a 25 m × 0.53 mm CarboPLOT P7 columm in a Varian GC 3800 equipped with a thermal conductivity detector. Helium was used as carrier gas. The composition of the condensed mixture (unconverted methanol and water) was analysed by a second gas chromatograph (Intersmat IGC 120 mL) using a 50 m × 0.53 mm fused Silica PLOT CP-Wax 58 (FFAP).

3. Results and discussion

3.1. Catalyst characterisation

3.1.1. X-ray diffraction

The XRD pattern of an "as prepared" sample mixed with 50 wt% corundum as internal standard is shown in figure 1. All XRD lines detected correspond to tetragonal (or cubic) zirconia, ZrO_2. The fact that ZrO_2 crystallises as a high temperature polymorph instead of the room temperature thermodynamically stable monoclinic form could be explained by either copper doping or particle size effects. The latter explanation is adopted here because our EXAFS analysis yields no evidence for copper incorporation into the zirconia lattice (see below). The XRD lines are significantly broadened due to small crystallite sizes, making it difficult to assess the degree of tetragonality. Assuming a narrow and uniform distribution, the average crystallite size can be estimated to be in the order of ~60 Å based on the Scherrer formula. By comparison of the peak intensities with the internal standard, the crystallinity of ZrO_2 is close to 100%, thus excluding a significant fraction of X-ray amorphous zirconia. Furthermore, the XRD pattern exhibits no peaks belonging to monoclinic ZrO_2. Due to the low copper content of the sample, an extremely weak CuO 111 peak is the only detectable sign of a copper containing phase. Upon reduction of the sample in 2% hydrogen at 250 °C, the XRD pattern changes slightly. In addition to the ZrO_2 peaks, the strongest reflection of metallic copper (Cu 111) becomes detectable.

3.1.2. X-ray absorption spectroscopy

The CuK edge spectrum of the calcined catalyst resembles that of copper(II) oxide CuO, but exhibits a pronounced reduction in amplitude (figure 2). An EXAFS refinement of a CuO model structure to the experimental spectrum resulted in a very good agreement between theoretical and experimental data, confirming that the copper containing phase of the catalyst is indeed CuO (figure 3). Furthermore, the quality of the fit allows us to exclude the presence of significant amounts of other copper phases, including copper incorporated into the ZrO_2 structure. The considerable amplitude reduction of the experimental spectrum was accounted for by a small Debye temperature (corresponding to large Debye–Waller factors) for the CuO model structure. Since the spectrum was taken at room temperature, this indicates a significant amount of disorder in the CuO structure and/or very small particle sizes. The EXAFS analysis of the reduced Cu/ZrO_2 sample shows that the reduction of CuO to Cu is complete within the limit of detection, again yielding no indication for copper doping of the zirconia structure. A more detailed structural study on this catalyst system will be presented elsewhere [A. Szizybalski, in preparation].

3.2. Catalytic measurements

In order to activate the catalyst, the initially present copper(II) oxide has to be reduced to metallic copper.

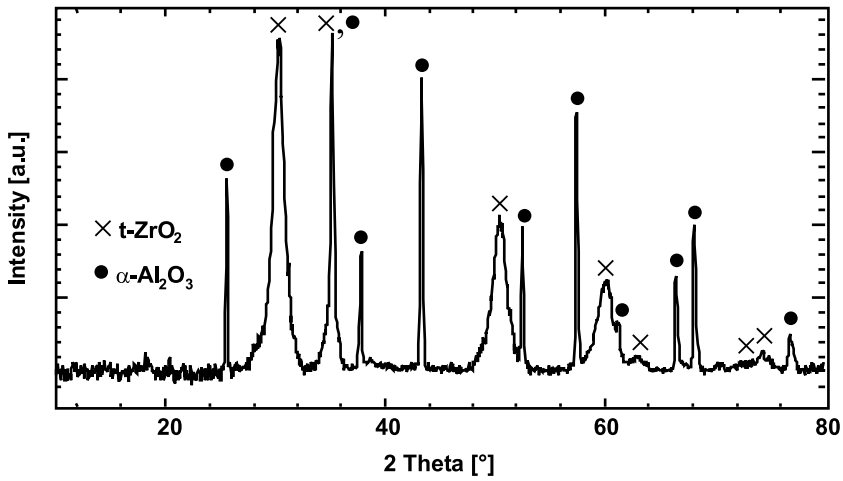

Figure 1. X-ray diffraction pattern of the CuO/ZrO_2 catalyst mixed with 50 wt% corundum as internal standard.

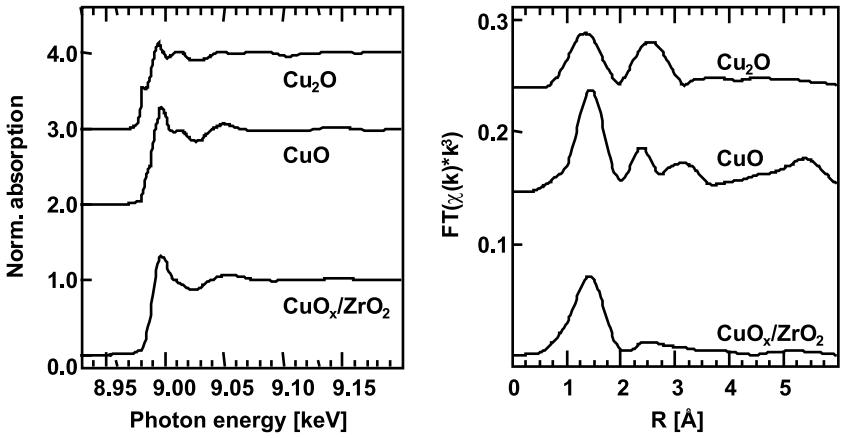

Figure 2. CuK-edge X-ray absorption spectra and radial distribution functions of the calcined catalyst (CuO/ZrO_2) and two reference samples (Cu_2O, CuO).

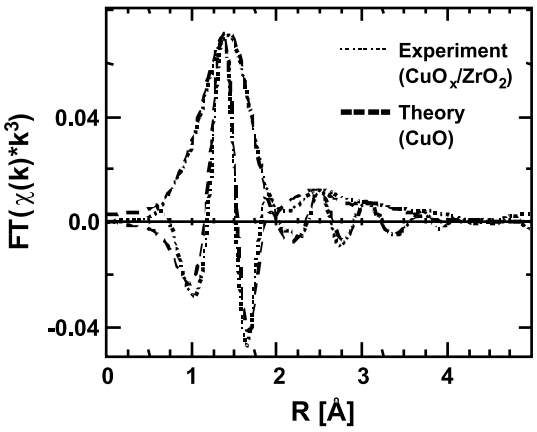

Figure 3. EXAFS fit of a CuO structure model to the experimental fourier transformed χ(k) of CuO/ZrO_2.

Possible treatments would be: (i) direct reduction by the methanol-water feedstock with methanol as the reducing agent or (ii) previous reduction in diluted hydrogen (e.g. 2%–5% H_2 in N_2). The influence of the different reduction treatments of the catalyst on the activity in methanol steam reforming has been studied by Idem and Bakhshi [26]. It was demonstrated that all Cu–Al catalysts without promoter and catalysts containing the optimum promoter (Mn, Cr, Zn) achieved higher methanol conversion when reduced in a methanol–water mixture than those initially reduced in a H_2 atmosphere. In our present work, reduction of the catalysts with methanol-water vapour at 250 °C was used for all experiments. The catalyst activity was evaluated in terms of methanol conversion (vol%). In order to evaluate the activity and selectivity behaviour of the Cu/ZrO_2 catalyst, a commercial $Cu/ZnO/Al_2O_3$ methanol synthesis catalyst (Süd-Chemie, approximately 50 wt% Cu) was examined at the same reaction conditions.

3.2.1. Activation behaviour

Figure 4 shows that the activity of the CuO/ZrO_2 catalyst can be increased significantly by temporary addition of oxygen to the feed (50 mL/min for 5 min). However, it is also apparent that the timing of the

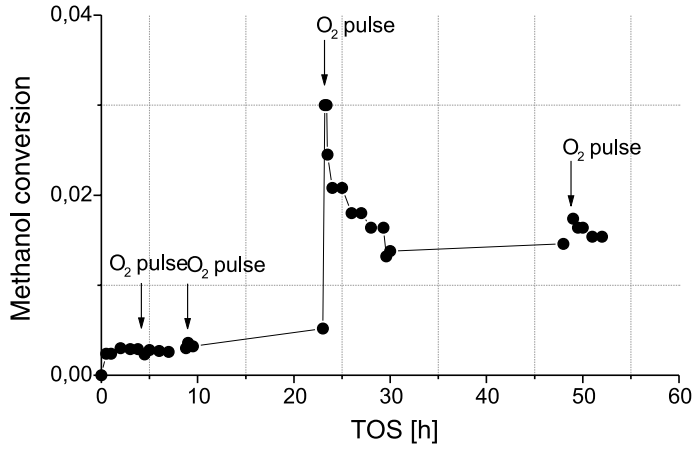

Figure 4. Activation of Cu/ZrO_2 catalyst by introducing O_2 into the feed. Reaction conditions: methanol/water molar ratio 1, T = 250 °C, flow rate of methanol/water mixture = 0.07 mL/min, mass of catalyst = 150 mg.

oxygen addition is an important factor. Initially, the catalyst is only slightly active after reduction in the feed. There is a slight increase in activity with time on stream. Oxygen additions during the first few hours have no apparent influence. In contrast, a drastic increase in activity is initiated by introducing oxygen after a longer time on stream. This sudden activity jump is followed by an approximately exponential decrease that ends at a higher activity level than before the oxygen addition. Another addition of oxygen several hours later causes only a small activity spike but no long term enhancement.

Because the beneficial effect of oxygen addition seems to depend on long time on stream, a similar experiment was performed on a larger time scale (more than 500 h, figure 5). It seems that the necessary time intervals between "successful" oxygen treatments increase continuously. The last oxygen addition, applied about 200 h after the previous last (very effective) addition, resulted in no further improvement. We concluded that the catalyst had reached its final and stable activity. Consequently, all further experiments on Cu/ZrO_2 described in the following sections were performed with the catalyst in this final state.

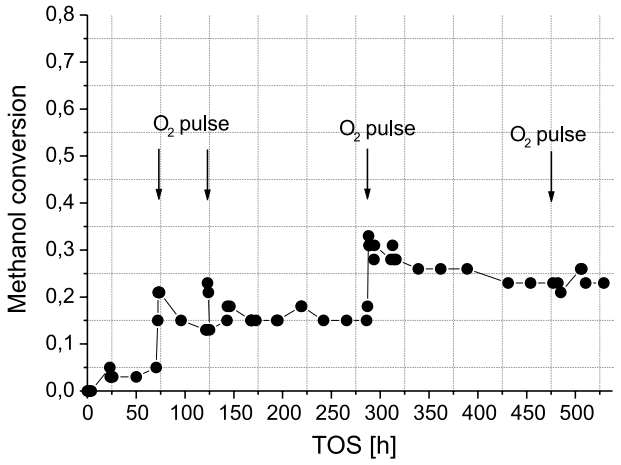

Figure 5. Activation of Cu/ZrO_2 catalyst by introducing O_2 into the feed. Reaction conditions: methanol/water molar ratio 1, $T = 250$ °C, flow rate of methanol/water mixture = 0.07 mL/min, mass of catalyst = 300 mg.

In order to study whether the catalyst activation is a reversible process or not, the reactor was cooled down to room temperature and opened at the end of one experiment, exposing the catalyst to air. Several days later, the reactor was closed again and reaction conditions were applied. After a short start-up time (re-reduction in the feed), the methanol conversion returned to about the same value as before the cool-down. This indicates that the activation procedure is an irreversible process.

It seems likely that the activation via oxygen treatment includes the formation of structural defects, which results in an increased catalytic activity. In a previous study [27], we were able to show that the activity of the CuO/ZnO catalyst system depends strongly on defects in the copper metal bulk structure, such as strain induced by the Cu/ZnO interface, or zinc dissolved in copper due to the preparation conditions. Structure–activity correlations for the Cu/ZrO_2 catalyst described here, particularly bulk structural changes during the oxygen treatment, are described elsewhere [A. Szizybalski, in preparation].

3.2.2. Catalytic activity

The contact time was varied by changing the liquid flow rate of the methanol water mixture between 0.02 and 0.2 mL/min. Figure 6 shows the methanol conversion as a function of W_{Cu}/F_m, with W_{Cu} indicating the mass of copper and F_m the flow rate of methanol. The CuO/ZrO_2 catalyst is found to be more active than the commercial $CuO/ZnO/Al_2O_3$ catalyst. Another comparison of the activity of $CuO/ZnO/Al_2O_3$ and CuO/ZrO_2/

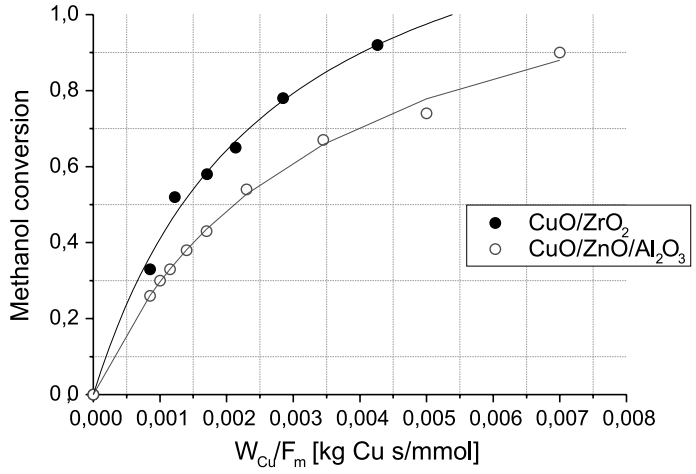

Figure 6. Comparison of activity between CuO/ZrO_2 catalyst and $CuO/ZnO/Al_2O_3$ catalyst. Methanol conversion versus W_{Cu}/F_m ratio (W_{Cu}: mass of copper).

Al_2O_3 catalysts has been carried out by Menon and co-workers [4]. Varying the copper loading from 3 to 12 wt%, they found that the $CuO/ZrO_2/Al_2O_3$ catalysts were significantly less active than the corresponding $CuO/ZnO/Al_2O_3$ catalysts. This discrepancy between our result and those reported by Menon and co-workers can be attributed to (i) the difference in the preparation methods of the CuO/ZrO_2 catalysts (polymer templating technique versus wet impregnation [28]) and (ii) the activation procedure described above.

3.2.3. Stability of the catalyst

One of the main problems using a $CuO/ZnO/Al_2O_3$ catalyst in SRM is the deactivation with time on stream. The experiment presented in figure 7 shows the methanol conversion as a function of time on stream for both CuO/ZrO_2 and $CuO/ZnO/Al_2O_3$. In order to compare the stability of both catalysts, the measurement was performed at similar reaction conditions, i.e. dilution of the catalyst with inert material and loading of the catalyst in the reactor. The deactivation of the catalysts with time on stream can be divided into two sections, (i) 0–100 h, the methanol conversion is decreasing non-linearly, (ii) >100 h linear behaviour. The decrease of the activity in the first section is more rapid than that at time on stream larger than 100 h. At the initial period (0–100 h), the deactivation of the CuO/ZrO_2 catalyst looks similar to that of the $CuO/ZnO/Al_2O_3$ catalyst. However, after more than 150 h, the methanol conversion is decreasing steadily for the $CuO/ZnO/Al_2O_3$ catalyst, while it appears to be constant for the CuO/ZrO_2 catalyst. The initial exponential decay of activity observed for both catalysts agrees with observations made by Löffler *et al.* on $CuO/ZnO/Al_2O_3$/graphite [29]. The authors studied the deactivation of several commercial water–gas shift catalysts in the methanol steam reforming reaction over more than 2000 h time on stream. Two simplified models for the deactivation rate were derived, based on (i) deactivation by metal sintering, and (ii) deactivation by feed poisoning, respectively. With the time dependence of the two models being significantly different (decreasing versus increasing rate of deactivation), the exponential decay observed for several catalysts was attributed to metal sintering. Following this interpretation, the smaller extent of deactivation of our CuO/ZrO_2 catalyst compared to commercial $CuO/ZnO/Al_2O_3$ seen in figure 7 indicates that the copper particles in the zirconia catalyst are less prone to sintering.

3.2.4. CO formation

The presence of CO in the product stream of SRM is a crucial problem for the use of the resulting hydrogen gas in a fuel cell, because adsorption of CO on the Pt electrode will deteriorate the polymer electrolyte fuel-cell performance [30]. In a previous report, we have shown that during the SRM over a commercial $CuO/ZnO/Al_2O_3$ catalyst, CO is formed as a consecutive product by the reverse water-gas shift reaction [31]. In addition, we were able to propose practical solutions for minimising the formation of CO. Figure 8 shows the CO production as a function of W_{cat}/F_m ratio for the CuO/ZrO_2 catalyst. The CO concentration, measured as volume content in the dry product stream, increases monotonically with increasing W_{cat}/F_m ratio for all temperatures. The S-shape of the curves indicates that CO, again, is formed as a consecutive product. Therefore, the reaction pathway of CO formation may be the same for copper based catalysts independent of the support type or synthesis method. Figure 8 also shows that the CO concentration increases with higher reaction temperatures at constant contact time. When the CO concentration is plotted as a function of the methanol conversion, an exponential increase is obtained in the observed temperature range (figure 9). In figure 10, the same representation is used to compare the CuO/ZrO_2

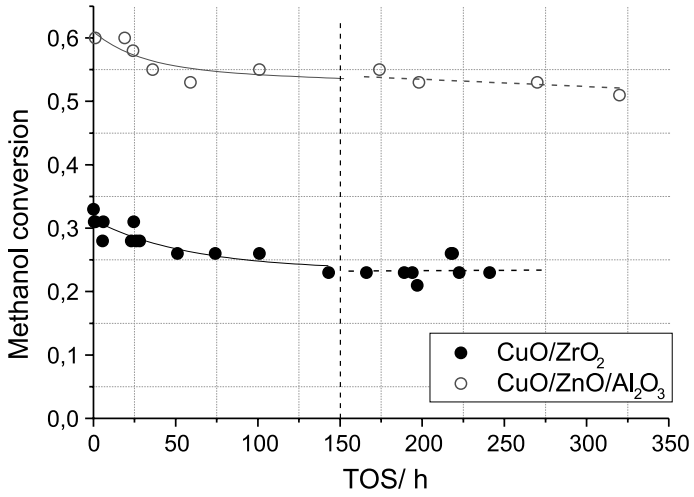

Figure 7. Deactivation experiment with CuO/ZrO_2 catalyst and $CuO/ZnO/Al_2O_3$ catalyst at comparable reaction conditions.

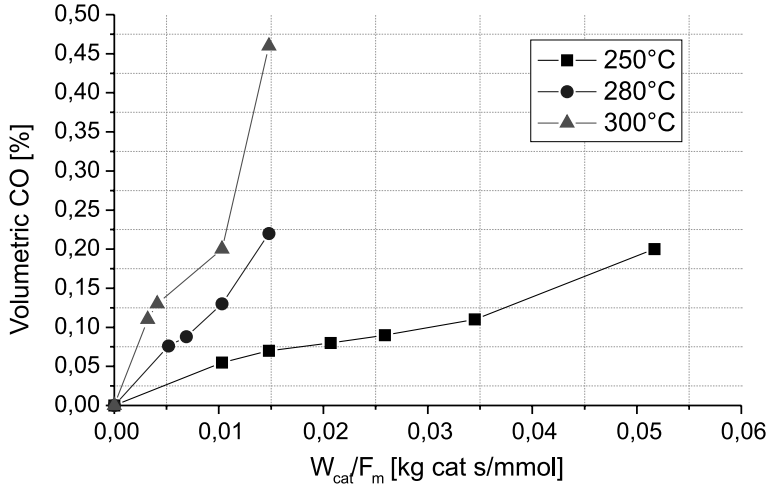

Figure 8. CO concentration as a function of W_{cat}/F_m ratio. Mass of the catalyst (CuO/ZrO_2) = 300 mg.

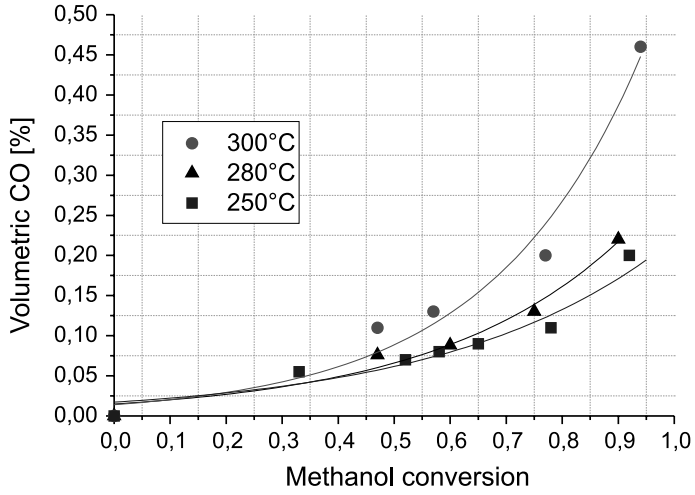

Figure 9. CO concentration as a function of methanol conversion. Mass of the catalyst (CuO/ZrO_2) = 300 mg.

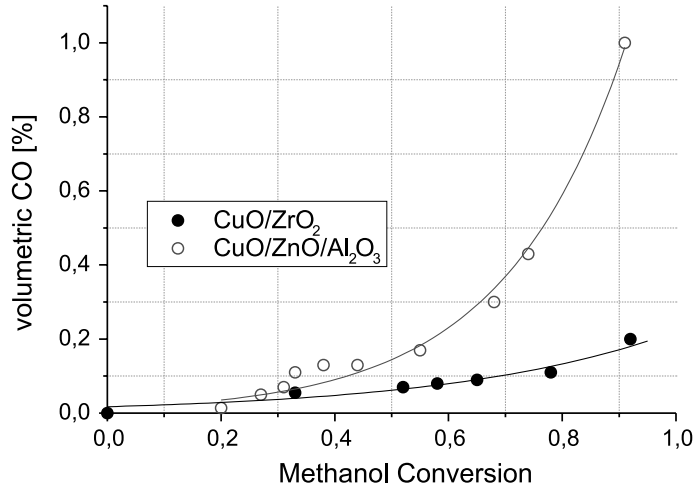

Figure 10. CO concentration in dependence on methanol conversion at 250 °C.

catalyst with $CuO/ZnO/Al_2O_3$ at 250 °C. It can be seen that CuO/ZrO_2 produces significantly less CO than the commercial catalyst at high conversions.

4. Conclusion

The catalytic properties of a novel CuO/ZrO_2 catalyst in the methanol steam reforming process were investigated at a temperature range from 250 to 300 °C at atmospheric pressure. The XRD and XAS results revealed that the CuO/ZrO_2 sample consists of small and/or disordered CuO particles and small particles of crystalline, tetragonal ZrO_2. The CuO/ZrO_2 catalyst can be activated by introducing oxygen (50 mL/min) for a short time (5 min) into the feed at reaction condition. The data obtained from contact time variation reveals that CO is produced as a consecutive product, as already has been demonstrated for $CuO/ZnO/Al_2O_3$. The new CuO/ZrO_2 catalyst, which was prepared by a polymer template sol–gel method, exhibits the following enhanced catalytic properties in comparison to the commercial $CuO/ZnO/Al_2O_3$ catalyst: (i) higher activity in terms of methanol conversion as a function of W_{Cu}/F_m, (ii) increased long term stability (i.e., less deactivation), probably because the macroporous zirconia support is more effective than ZnO/Al_2O_3 in preventing copper particle sintering, and (iii) reduced CO formation, especially significant at high methanol conversion. Our work shows clearly that a knowledge-based preparation of heterogeneous catalysts is feasible permitting the rational design of materials exhibiting an improved catalytic performance. Elucidating structure–activity relationships is a necessary prerequisite for a rational catalyst design, however, detailed knowledge about appropriate preparation and treatment conditions resulting in the right target structure of the heterogeneous catalyst is equally important.

References

[1] L.F. Brown, Int. J. Hydrogen Energy 26 (2001) 381.
[2] J. Agrell, H. Birgersson and M. Boutonnet, J. Power Sources 106 (2002) 249.
[3] S. Velu, K. Suzuki, M.P. Kapoor, F. Ohashi and T. Osaki, Appl. Catal. 213 (2001) 47.
[4] B. Lindström, L.J. Petterson and P.G. Menon, Appl. Catal. 234 (2002) 111.
[5] M.L. Cubeiro and J.L.G. Fierro, Appl. Catal. 168 (1998) 307.
[6] Y. Choi and H.G. Stenger, Appl. Catal. B: Environ. 38 (2002) 259.
[7] W. Ning, H. Shen and H. Liu, Appl. Catal. A: Gen. 211 (2001) 153.
[8] H.A. Gasteiger, N. Markovic, P.N. Ross and E. Cairs, J. Phys. Chem. B 98 (1994) 617.
[9] V.M. Schmidt, P. Brocherhoff, B. Hohlein, R. Menzer and U. Stimming, J. Power Sources 144 (1994) 175.
[10] R.O. Idem and N.N. Bakhshi, Can. J. Chem. Eng. 74 (1996) 288.
[11] J. Agrell, K. Hasselbo, K. Jansson, S.G. Järas and M. Boutonnet, Appl. Catal. A: Gen. 211 (2001) 239.
[12] G.C. Shen, S. Fujita, S. Matsumoto and N. Takezawa, J. Mol. Catal. A: Chem. 124 (1997) 123.
[13] B. Lindström and L.J. Pettersson, Int. J. Hydrogen Energy 26 (2001) 923.
[14] C.J. Jiang, D.L. Trimm and M.S. Wainwright, Appl. Catal. A: Gen. 93 (1993) 245.
[15] B. Lindström and L.J. Pettersson, J. Power Sources 106 (2002) 264.
[16] R.O. Idem and N.N. Bakhshi, Chem. Eng. Sci. 51 (1996) 3697.
[17] J.P. Breen and J.R.H. Ross, Catal. Today 51 (1999) 521.
[18] M. Antonietti and H.-P. Hentze, Colloid Polym. Sci. 274 (1996) 696.
[19] M. Antonietti and H.-P. Hentze, Adv. Mater. 8 (1996) 840.
[20] M. Antonietti, R.A. Caruso, C.G. Göltner and M.C. Weissenberger, Macromolecules 32 (1999) 1383.
[21] H.-P. Hentze and M. Antonietti, Curr. Opin. Solid St. Mater. Sci. 5 (2001) 343.
[22] R.A. Caruso, M. Giersig, F. Willig and M. Antonietti, Langmuir 14 (1998) 6333.
[23] J.H. Schattka, D.G. Shchukin, J. Jia, M. Antonietti and R.A. Caruso, Chem. Mater. 14 (2002) 5103.
[24] T. Ressler, J. Synch. Rad. 5 (1998) 118.
[25] J.J. Rehr, C.H. Booth, F. Bridges and S.I. Zabinsky, Phys. Rev. B 49 (1994) 12347.
[26] R.O. Idem and N.N. Bakhshi, Ind. Eng. Chem. Res. 34 (1995) 1548
[27] M.M. Günter, T. Ressler, R.E. Jentoft and B. Bems, J. Catal. 203 (2001) 133.
[28] E.D. Guerreiro, O.F. Gorriz, G. Larsen and L.A. Arrúa, Appl. Catal. A 204 (2000) 33.
[29] D.G. Löffler, S.D. McDermott and C.N. Renn, J. Power Sources (2002) 5063.
[30] K. Narusawa, M. Hayashida, Y. Kamiya, H. Roppongi, D. Kurashima and K. Wakabayashi, JSAE Rev. 24 (2003) 41.
[31] H. Purnama, T. Ressler, R.E. Jentoft, H. Soerijanto, R. Schlögl and R. Schomäcker, Appl. Catal. A., in press.